The Gulf Stream and Its Frontal Structure: A Quantitative Representation

TIMOTHY W. KAO

Department of Civil Engineering, The Catholic University of America, Washington, DC 20064

(Manuscript received 26 February 1986, in final form 26 July 1986)

ABSTRACT

The structure of the Gulf Stream Current is associated with the quasi-permanent density front in the western North Atlantic. The lighter mass of warmer but saltier water of the Sargasso Sea is separated from the slope water by inclined isopycnals that form the front. Recent satellite altimeter measurements have also revealed a well-defined sea-surface height change across the front. In this paper, a model of the Gulf Stream cross-sectional density and current structure is presented, using the complete dynamical and mass-conservation equations. The model postulates a forcing, at the interior ocean boundary, by a cross-stream ageostrophic circulation with inflow of light water in the upper ocean and a return flow at greater depths. The model Gulf Stream is found to develop after initial geostrophic adjustment of several inertial periods.

In the quasi-steady state, the normalized structural results constitute a single representation of the structure of all Gulf Stream sections; i.e., all sections are similar. The normalization requires only two observational inputs: (i) either a suitably defined depth of a representative isopycnal in the main pycnocline beneath the Sargasso Sea or the total sea-surface height change across the front, and (ii) the maximum downstream surface velocity of the Stream. The model can therefore be used to produce the entire cross-sectional structure of the Gulf Stream and its front from simple and limited observational inputs.

The results are compared with representative field data from (i) the Gulf Stream '60 experiment, (ii) the Seasat altimeter experiment, and (iii) the recent Gulf Stream Current measurements by the University of Rhode Island group using the Pegasus current profiler. Quantitative agreement between the model results and the field data is found.

1. Introduction

An important new tool for the study of upper-ocean dynamics is the use of satellite altimetry of high accuracy. Almost instantaneous overflies of large distances become routinely possible. When an accurate geoid is also available, the sea-surface height variations along a track become readily obtainable. The question is then the following: from the sea-surface height variations, is it possible to solve the inverse problem of the subsurface density field and hence, through geostrophy, the baroclinic current structure and transport? Obviously, this inverse problem is not uniquely determinable without sufficient "prior data." The sufficient conditions for uniqueness also depend on the ocean dynamics of interest as well as on the manner in which the problem is posed. Equally obvious is the desirability and usefulness of the solution of such an inverse problem in monitoring continuously and remotely the ocean circulation.

A realistic strategy for generating the "prior data" appears to involve dynamical modeling, self-coherent past information, and limited in situ measurements. On a global scale, such a strategy awaits future developments in all of these aspects. However, on a more regional basis, in particular for the Gulf Stream (GS), this strategy can be made practical with a realistic frontal model of the GS, the specification of minimum requirements on concurrent in situ measurements dictated by the model, and the known tight correlation of the isopycnals and certain isotherms in the GS.

In this paper we give the results of a quasi-steady-state Gulf Stream model. We will make quantitative comparisons with three different datasets of the Gulf Stream and show how the model would be used for the solution of the inverse problem within limits. The model is a modified version of a frontal model previously proposed by Kao (1980). In that model, the front has a steady forward motion that has to be brought to zero by adding a uniform flow. Furthermore, it lacks the thermocline structure in the slope-water side of the front, and thus it cannot be quantitatively compared with the existing hydrographic data.

It should be pointed out that the model is a frontal model in contrast to the more conventional basinwide two- or three-layer models (e.g., see Hurlburt, 1984). It attempts to seek a basic understanding of the dynamics of the maintenance of the Gulf Stream front, while functioning as a diagnostic tool. The emphasis of the model is on the detailed cross-sectional structure of the Gulf Stream front, and hence it deals only with the baroclinic aspects of the Gulf Stream.

2. The model

The model is based on the numerical integration of the full Navier–Stokes and diffusion equations in a vertical cross-stream plane. The model is two-dimen-

sional in that the flow is independent of the downstream direction, even though all three components of motion are present. The model postulates a forcing by an ageostrophic inflow of light water in the upper ocean and a return flow at greater depths. In the integration scheme, an initial value problem is posed in which an inflow Q_e (per unit length along the downstream direction y^*) of light water was introduced into an ambient stratified fluid initially at rest. The ambient density, $\bar{\rho}_0(z^*)$, varies linearly in the vertical direction, z^*, in the upper layers and is a constant, ρ_0, below. Specifically, we take a rectangular region in the x^*–z^* plane as our domain of integration, with the cross-stream distance x^* extending from 0 to $-\infty$ and z^* from 0 to some finite depth $-d$. The inflow–outflow takes place on the boundary $x^* = 0$ and normal to it, with a zero net volumetric discharge across $x^* = 0$. The horizontal surface and bottom are stress-free, insulated, and have no flow across them. There is no motion at $x^* = -\infty$. The initial forcing consists of a set of baroclinic modes represented by the initial streamfunction, nondimensionalized by Q_e,

$$\Psi_0 = \sum_{k=1}^{\infty} f(k) \exp(k\pi x) \sin k\pi(z+1)$$

where $(x, y, z) = (x^*, y^*, z^*)/d$, and $f(k)$ is determined so that Ψ_0 satisfies the boundary condition at $x = 0$ that the inflow velocity is uniform from $z = z_1$ to $z = 0$ and the outflow velocity is uniform from $z = z_1$ to $z = -1$, where z_1 is any point in the interval $(-0.2, -0.1)$,

$$\Psi = \begin{cases} z\left(\dfrac{1+z_1}{z_1}\right), & z_1 < z < 0 \\ z+1, & -1 < z < z_1. \end{cases}$$

The inflow has a density deficit $(\Delta\rho)_e$ relative to the bottom water of density ρ_0. If the velocities are normalized by Q_e/d, we denote $(u, v, w) = (u^*, v^*, w^*)/(Q_e/d)$ to be the dimensionless velocities in x, y, z directions, respectively, and $u = \partial\Psi/\partial z$, and $w = -\partial\Psi/\partial x$.

In an f-plane frame of reference, the governing equations are given below in nondimensional form:

$$\frac{\partial\gamma}{\partial t} + \frac{\partial}{\partial x}(u\gamma) + \frac{\partial}{\partial z}(w\gamma) = \frac{1}{\mathrm{ScRe}}\nabla^2\gamma. \tag{1}$$

Equation (1) represents the diffusion equation of the density deficit γ, where $\gamma = (\rho - \rho_0)/\rho_0$; Sc is the Schmidt number, which is the ratio of the eddy viscosity ν to the diffusion coefficient; Re is the Reynolds number and is equal to Q_e/ν; and $\nabla^2 \equiv \partial^2/\partial x^2 + \partial^2/\partial z^2$.

$$\frac{\partial\zeta}{\partial t} + \frac{\partial}{\partial x}(u\zeta) + \frac{\partial}{\partial z}(w\zeta) - \frac{1}{\mathrm{Ro}}\frac{\partial v}{\partial z} = \frac{1}{F^2}\frac{\partial\gamma}{\partial x} + \frac{1}{\mathrm{Re}}\nabla^2\zeta. \tag{2}$$

Equation (2) is the equation governing the y-component of vorticity ζ, where Ro is a Rossby number given by $Q_e/(fd^2)$ and F is a Froude number given by $Q_e/(gd^3)^{1/2}$, where g is the acceleration of gravity. Now,

$$\zeta = \frac{\partial u}{\partial z} - \frac{\partial w}{\partial x} = \nabla^2\Psi \tag{3}$$

through the continuity equation.

$$\frac{\partial v}{\partial t} + \frac{\partial}{\partial x}(uv) + \frac{\partial}{\partial z}(wv) + \frac{1}{\mathrm{Ro}}u = \frac{1}{\mathrm{Re}}\nabla^2 v. \tag{4}$$

Equation (4) is the equation of motion for the downstream velocity v.

In the numerical integration of the above set of equations with the boundary conditions stated earlier, we assume the equality of the eddy viscosity and diffusivity so that Sc = 1. Obviously, there remains an extremely large parametric regime for the solutions. It was, however, shown in Kao that the parametric regime can be narrowed considerably by scaling considerations. Equations (1) through (4) can be rescaled, neglecting terms of order ϵ^2, where ϵ is the small parameter defined in (8) below, to a set of evolutionary equations that depend only on a single parameter, E, an Ekman number. This was defined as the ratio of the Ekman layer thickness (ν/f) to the vertical buoyancy scale, h_0, where $h_0 = (Q_e^2/g')^{1/3}$ and

$$g' = \frac{(\Delta\rho)_e}{\rho_0} g. \tag{5}$$

For the Gulf Stream frontal region, E was estimated to be small; i.e., the frictional effect was small. Furthermore, the solutions to the governing equations were found in Kao to be insensitive to variations in E for sufficiently small values of E, and $E = 0.025$ was determined to be representative.

The main changes in the present model from the model in Kao are the introduction of the initial ambient stratification and the modification of the inflow–outflow boundary condition so that the cross-stream circulation is imposed ab initio, making it unnecessary to add a uniform flow to arrest the front. The scaling arguments and the rescaled governing equations, presented in Kao, however, remain the same and will not be repeated here. For the sake of clarity, we list below the relevant scales and parameters. The horizontal velocity scale is given by

$$U_d = (g'Q_e)^{1/3}. \tag{6}$$

The time scale is given by the inertial time,

$$T = 1/f. \tag{7}$$

From (6) and (7), we obtain an internal radius of deformation, L_0, where $L_0 = U_d/f$. The ratio h_0/L_0 is a representative slope of the inclined isopycnals of the front and is denoted by ϵ, i.e.,

$$\epsilon = \frac{h_0}{L_0} = \left[\frac{Q_e}{(g')^2}\right]^{1/3} f. \tag{8}$$

(Note that in Kao, ϵ was denoted by $1/\tilde{R}_0$.) The values of ϵ are $O(10^{-2})$ or less in problems of oceanographic interest.

In summary, the basic element in the present model is a recirculating ageostrophic flow in the cross-stream direction, characterized by the inflow of light water of Q_e per unit downstream length. The model is therefore different from the regional quasi-geostrophic multilayer models, which are inappropriate in the frontal region. The present model is started as an initial value problem and achieves a quasi-steady state after initial geostrophic adjustment. The model results for the quasi-steady state are the ones that will be presented.

3. Results and discussions

A quasi-steady state is achieved after initial geostrophic adjustment of several inertial periods. (The parameters chosen for these calculations are $F^2 = 3 \times 10^{-6}$, Re = 400, and Ro = 10^{-1}, so that $E = 0.025$.) In that state it is found that the following balances, stated in terms of the rescaled equations of Kao, are achieved: (i) advective–diffusive balance,

$$\frac{\partial(\tilde{u}\tilde{\gamma})}{\partial\xi}+\frac{\partial(\tilde{w}\tilde{\gamma})}{\partial\eta}=E\frac{\partial^2\tilde{\gamma}}{\partial\eta^2}, \tag{9}$$

where $(\tilde{u}, \tilde{v}, \tilde{w}) = (u^*, v^*, w^*/\epsilon)/U_d$, $(\xi, \eta) = (x^*/L_0, z^*/h_0)$, and $\tilde{\gamma}$ is γ normalized by γ of the inflow; (ii) thermal wind balance,

$$-\frac{\partial\tilde{v}}{\partial\eta}=\frac{\partial\tilde{\gamma}}{\partial\xi}; \tag{10}$$

and (iii) advective–Coriolis balance

$$\frac{\partial(\tilde{u}\tilde{v})}{\partial\xi}+\frac{\partial(\tilde{w}\tilde{v})}{\partial\eta}+\tilde{u}=0 \tag{11}$$

for the downstream component of momentum. The importance of the nonlinear terms in the first and third of the balances should be noted.

As a reference, the model was also run for the case of an unstratified ambient. As expected, the results were not substantially different from the stratified case except for the near-surface density structure on the cyclonic (left-hand) side of the velocity core. Those results, therefore, will not be presented here.

In the quasi-steady state, we let $\bar{D}$ denote the depth of an isopycnal that is one-tenth the total density difference $(\Delta\rho)_e$ between the light water pool and the deep heavier water. We let $\bar{L}$ be the width of the Stream, defined as the distance from the inflow–outflow boundary, $x^* = 0$, to a point at the surface on the cyclonic side of the velocity core, where the downstream velocity is equal to two-tenths of the maximum downstream velocity, v_m^*. (See Figs. 1a and 1b.) (The $\bar{L}$, so defined, is also the horizontal location at the surface of the bounding isopycnal of one-tenth $(\Delta\rho)_e$ in the corresponding unstratified case.) It is then found from the model results that $\bar{D}/\bar{L}$ is proportional to ϵ. In fact, it is found that

$$\bar{L}/\bar{D}=(2.27\epsilon)^{-1} \tag{12}$$

and that the maximum downstream velocity v_m^* is

$$v_m^*=2.65U_d=2.65(g'Q_e)^{1/3}. \tag{13}$$

Thus, from (12), on using (8) and (13), we find that

$$\bar{L}=1.17\frac{g'\bar{D}}{fv_m^*}. \tag{14}$$

In addition, we find from the model results that the maximum sea-surface height change across the front, Δh_m, is given by

$$\Delta h_m=0.7(g'/g)\bar{D}. \tag{15}$$

The structural results to be given below will be normalized by $(\bar{L}, \bar{D}$, and $v_m^*)$. Under this normalization, the results constitute a single representation of the structure of all GS sections; i.e., all GS sections are similar. To gain further perspective, these results can also be viewed in the context of Stommel's (1965) simple, qualitative, two-layer model of the GS front. Stommel's model, of course, lacks the cross-stream circulation as well as the diffusional effect of the present model. Nevertheless, at this point it is useful to recall Stommel's model, which is based on two basic principles: (i) geostrophy, or

$$fv^*=g'\frac{\partial D}{\partial x^*}, \tag{16}$$

where D is the depth of the interface between the two layers, and (ii) the potential vorticity of the light water is uniform,

$$f+\frac{\partial v^*}{\partial x^*}=\frac{f}{D_0}D, \tag{17}$$

where D_0 is the asymptotic depth of the light water pool. From these principles we immediately obtain the results:

$$v^*=v_m^*\exp[-x^*/\lambda_s] \tag{18}$$

$$D=D_0[1-\exp(-x^*/\lambda_s)] \tag{19}$$

where $v_m^*=(g'D_0)^{1/2}$ is the maximum downstream Gulf Stream velocity and $\lambda_s = (g'D_0)^{1/2}/f$ is the internal Rossby radius of deformation. (Note that Stommel placed the origin of his x^*-axis at $D = 0$.)

It is clear that v_m^* and λ_s are not independent quantities, since λ_s is simply v_m^*/f. In the present model, on the other hand, v_m^* and $\bar{L}$ are independent quantities, with v_m^* depending only on $(g'Q_e)$ and $\bar{L}$ proportional to $\bar{D}/\epsilon$. Thus, from a practical point of view, Stommel's model has one single dimensional parameter $(g'D_0)$ whereas the present model has essentially two, namely, $(g'Q_e)$ and D.

To simplify comparison with field and altimetry data, another cross-stream length-scale, λ, was intro-

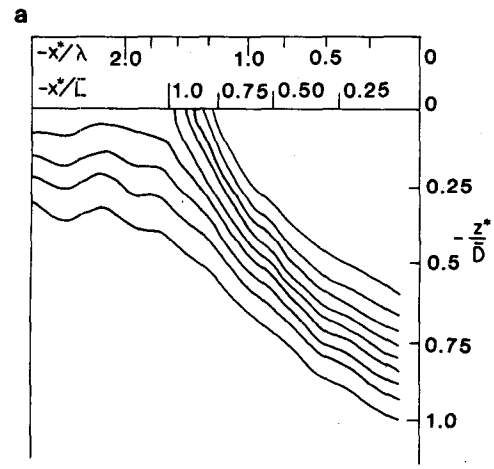

FIG. 1a. Model-generated frontal isopycnals. Each isopycnal represents $\frac{1}{10}$ the total density anomaly. Note the stretched coordinate in the cross-stream direction.

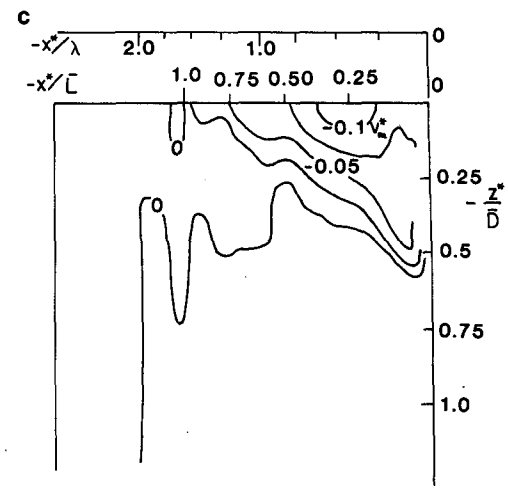

FIG. 1c. Model-generated isotachs of the cross-stream velocity. Each isotach represents $\frac{1}{20}$ of v_m^*. The maximum cross-stream velocity is $0.1v_m^*$. Note the stretched coordinate in the cross-stream direction.

duced by Kao and Cheney (1982). This length scale is given by

$$\lambda = \frac{g}{f}\frac{\Delta h_m}{v_m^*}. \tag{20}$$

Now, if $h(x)$ represents the sea-surface height variation across the front, v_m^* is also given by the usual geostrophic relationship,

$$v_m^* = \frac{g}{f}\left(\frac{dh}{dx}\right)_m \tag{21}$$

in which $(dh/dx)_m$ is the maximum slope of the sea-surface height profile. It is easily seen that in the model,

$$\bar{L} = 1.65\lambda. \tag{22}$$

Details of the structural results to be presented below will include the horizontal scale normalized by λ.

The model results for the isopycnals, the isotachs of the downstream velocity, the isotachs of the cross-stream velocity, and the streamlines of the cross circulation are shown in Figs. 1a, b, c, and d, respectively. The cross-stream coordinate is normalized by λ in the upper scale and by $\bar{L}$ in the lower scale. For comparison with field data, the upper scale is the preferred scale. (Note the exponential stretching in the cross-stream direction.) In Fig. 1a the isopycnals are displayed at intervals of one-tenth the total density anomaly between the light water and the deep heavier water. It shows a pool of light water separated from the slope water by inclined isopycnals that form the front. The light water mass is bounded below by the base of the main oceanic pycnocline. For definiteness, we identify the lowest isopycnic, which is one-tenth of the total

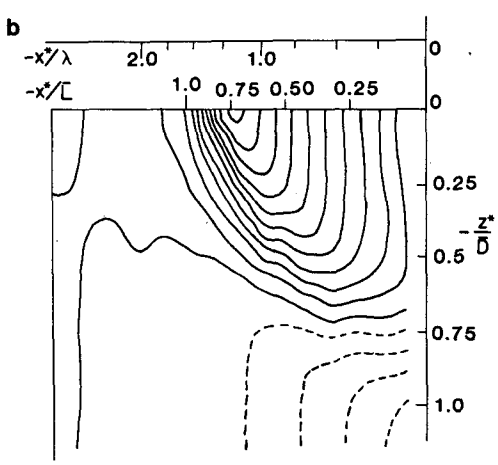

FIG. 1b. Model-generated isotachs of the downstream velocity. Each isotach is $\frac{1}{10}$ the maximum downstream velocity v_m^*. Note the stretched coordinate in the cross-stream direction.

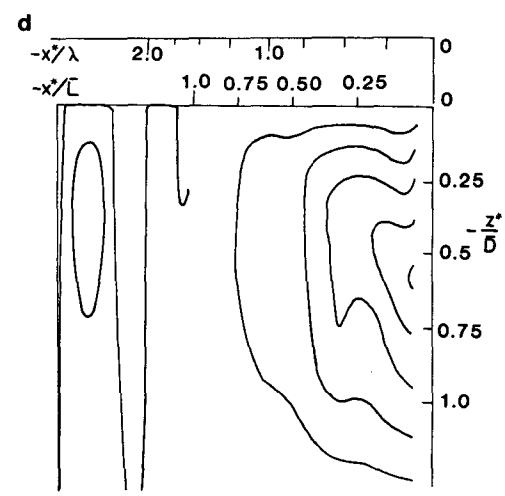

FIG. 1d. Model-generated streamline of the cross-stream velocity. Note the stretched coordinate in the cross-stream direction.

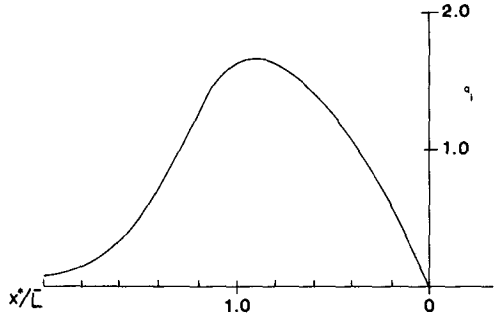

FIG. 2. Model-generated nondimensionalized downstream baroclinic transport per unit width, q_i, as a function of the cross-stream distance.

density anomaly, as the base of the main pycnocline. The isopycnals of the main pycnocline are tilted upward to form the frontal isopycnals. Nearer the free surface the inclined frontal isopycnals are joined to the near-surface pycnocline of the slope water. This frontal density structure is typical of the Gulf Stream front. The warmer, but saltier, water of the Sargasso Sea constitutes the light water pool.

In Fig. 1, the vertical coordinate is normalized by the depth $\bar{D}$ of the base of the main pycnocline as defined previously. Thus if, for example, $g' = 1.5 \times 10^{-2}$ m s^{-2}, $Q_e = 30$ m^2 s^{-1}, and $\bar{D} = 1400$ m, then $U_d = 0.77$ m s^{-1}, so that $v_m^* = 2.0$ m s^{-1} from (13), $\bar{L} = 123$ km from (14), $\epsilon = 0.005$ (on taking $f = 10^{-4}$ s^{-1}), and $\lambda = 75$ km from (22). It should be emphasized that all Gulf Stream sections are similar in this model, with the variations between different dimensional sections depending only on $(g'Q_e)$ and $\bar{D}$.

Figure 1b shows the isotachs of the downstream velocity spaced at equal intervals of one-tenth the maximum velocity. The position of maximum velocity is at the surface at $x^*/\bar{L} = -0.75$. The structure of the downstream velocity clearly exhibits the typical features of the Gulf Stream. An intense surface jet is present at the upper layer of the ocean. The intensity of the jet diminishes as the depth increases, with the point of maximum velocity shifting to the right (or toward the Sargasso Sea side). There is cyclonic (positive) horizontal shear on the left side of the jet and weaker anticyclonic shear on the right. It is seen from Fig. 1b that at the surface the cyclonic shear is about twice as strong as the anticyclonic shear. Strong vertical shear is present in the frontal region and zero vertical shear in the light water pool. Furthermore, the downstream velocity variation in the light water pool is exponential in the cross-stream direction, which shows that potential vorticity is conserved in the light water pool. (Note the uniformity of the isotach spacing in the light water pool in the exponentially stretched cross-stream coordinate.) For the example above, the cyclonic shear is approximately 0.5×10^{-4} s^{-1}, or half of f, and the vertical shear at the location of the maximum downstream velocity is 0.002 s^{-1}. It is also seen in the figure that, as part of the baroclinic current structure, an undercurrent is present at depths beneath the Stream as a result of the outflow boundary condition at depth.

Figure 1c shows the isotachs of the cross-stream velocity at intervals of $0.025v_m^*$. The cross-stream velocity is strongest at the surface with a maximum magnitude of one-tenth the downstream maximum velocity located in the light water pool. The cross-stream velocity decreases with depth and decreases to zero as it approaches the left edge of the downstream jet. Indeed, $x^*/\bar{L} = -1$ defines an almost vertical plane where the

TABLE 1. Model-generated quantities for different values of input parameters.

Input parameters		Model-generated quantities						
Q_e (m^2 s^{-1})	$\bar{D}$ (m)	v_m^* (m s^{-1})	u_m^* (m s^{-1})	$\bar{L}$ (km)	λ (km)	$(q_R)_m$ (m^2 s^{-1})	Q (Sv)	Δh_m (m)
10	1000	1.41	0.141	124	75	497	42	1.07
10	1400	1.41	0.141	174	105	698	82	1.50
10	1800	1.41	0.141	224	136	898	136	1.93
20	1000	1.77	0.177	99	60	626	42	1.07
20	1400	1.77	0.177	139	84	876	82	1.50
20	1800	1.77	0.177	178	108	1127	136	1.93
30	1000	2.03	0.203	86	52	718	42	1.07
30	1400	2.03	0.203	121	73	1005	82	1.50
30	1800	2.03	0.203	156	95	1292	136	1.93
40	1000	2.24	0.224	78	47	792	42	1.07
40	1400	2.24	0.224	110	67	1109	82	1.50
40	1800	2.24	0.224	141	85	1426	136	1.93
50	1000	2.41	0.241	73	44	852	42	1.07
50	1400	2.41	0.241	102	62	1193	82	1.50
50	1800	2.41	0.241	131	79	1534	136	1.93

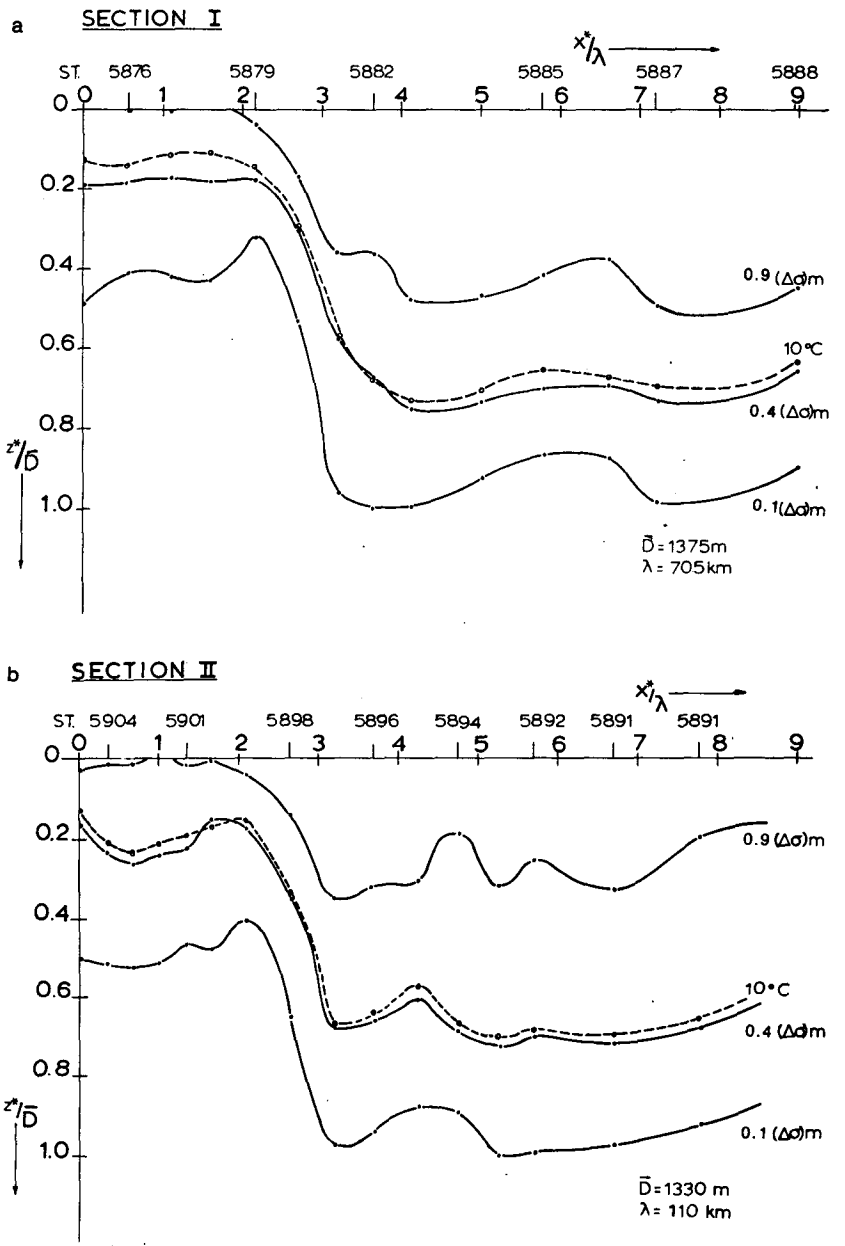

FIG. 3. (a) Isopycnals of section I of Gulf Stream '60 at 68°30'W with $\bar{D}$ = 1375 m. (λ = 70 km from model.) Fuglister's station numbers are shown. (b) Isopycnals of section II at 66°30'W with $\bar{D}$ = 1330 m. (λ = 110 km.) (c) Isopycnals of section III at 64°30'W with $\bar{D}$ = 1450 m. (λ = 91 km.)

cross-stream velocity is zero. There is thus a zone of horizontal convergence in the upper ocean toward the front. For the example above, the average convergence du^*/dx^* in the upper 400 m is approximately 1.5 $\times 10^{-6}$ s^{-1}.

Figure 1d shows the streamlines of the ageostrophic cross-stream circulation. It should be pointed out that although in the present computation x^* extends to $-\infty$, a rigid wall boundary condition can be imposed at any $|x^*/\lambda| > 2$ without affecting the results.

The upper ocean baroclinic transport of the jet can be readily evaluated by integrating the downstream velocity field. The result is shown in Fig. 2, where the transport per unit width, q_i, is plotted against the cross-stream distance, x^*/λ. The dimensional downstream transport per unit width can then be shown to be

$$q_R = 568 q_i U_d \bar{D} \text{ [m}^3 \text{ s}^{-1}\text{/km]} \quad (23)$$

and the total downstream baroclinic transport is found to be

$$Q = 0.28(g'\bar{D}^2/f) \times 10^{-6} \text{ Sv.} \quad (24)$$

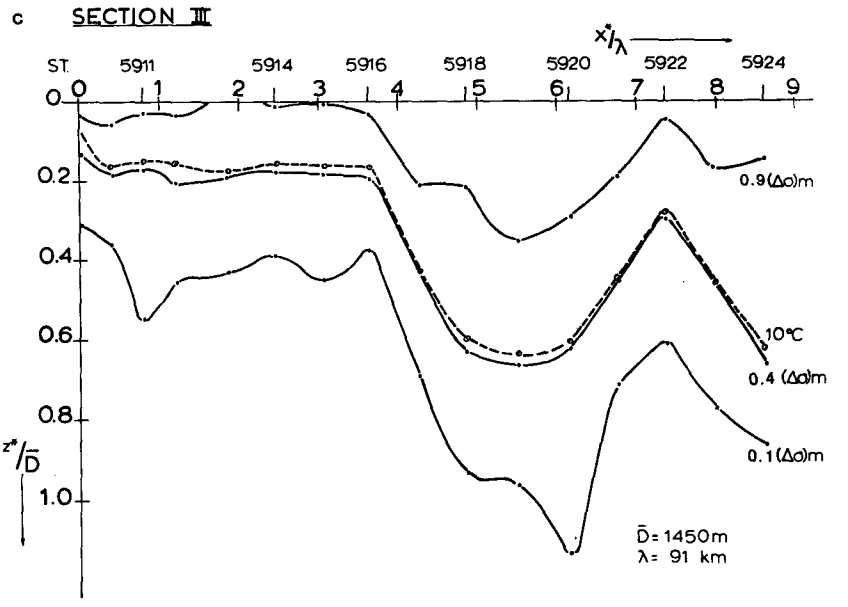

FIG. 3. (*Continued*)

where 1 Sv $\equiv 10^6$ m^3 s^{-1}. Again, for the example above, $q_R = 0.475 \times 10^6 q_i$ (m^3 s^{-1}/km) so that the maximum transport per unit width $(q_R)_m$ is 1.0×10^6 m^3 s^{-1} km^{-1} or 1000 m^2 s^{-1}, and the total downstream baroclinic transport Q is 82 Sv.

Table 1 gives the model-predicted values of the maximum downstream velocity, v_m^*; the maximum cross-stream velocity, u_m^*; the Gulf Stream width, $\bar{L}$; the width, λ; the maximum downstream transport per unit width, $(q_R)_m$; the total baroclinic downstream transport, Q; and the maximum sea-surface rise across the stream $(\Delta h)_m$ for various assumed values of Q_e and $\bar{D}$ with $g' = 1.5 \times 10^{-2}$ m s^{-2} and $f = 10^{-4}$ s^{-1}.

We are now in the position to make quantitative comparison with some existing field data of the Gulf Stream.

4. Quantitative comparison with field data

Quantitative comparisons with field data of the Gulf Stream structure will now be given for three different types of field results. The comparisons are by no means exhaustive, but they are nonetheless representative. The field data are taken from (i) the hydrographic data of Fuglister's Gulf Stream '60, (ii) altimetry data from Seasat, and (iii) the recent direct current data of Halkin and Rossby (1985) using the Pegasus. These three field data types are all taken at the same general geographical location northeast of Cape Hatteras and west of the New England Seamounts, i.e., west of 64°30'W.

For comparisons with the field data, f is taken to be 10^{-4} s^{-1} for that general region and g' is taken to be 1.5×10^{-2} m s^{-2} from an examination of historical hydrographic data of the region. With these values fixed, the only input parameters to the model are $(g'Q_e)$ and $\bar{D}$. Now $v_m^* = 2.65(g'Q_e)^{1/3}$ according to (13) and v_m^* can be obtained from the field data. Thus, v_m^* will be used instead of $(g'Q_e)$.

The general procedure for the comparisons is as follows.

1) From the field data, v_m^* and $\bar{D}$ or Δh_m are obtained.

2) From the model, $\bar{L}$, λ and Q_e are determined by the appropriate formulas.

3) The field data is normalized, the cross-stream distance by $\bar{L}$ (or λ), the depth by $\bar{D}$, and the sea-surface height change by Δh_m. The relevant structure is compared with the model results; in the case of data type (iii), the field-estimated value of Q_e will also be compared with the model-calculated value.

4) A reference point is assigned on the x^*-axis by identifying a well-defined feature of the Stream so that its geographical location varies with the location of the Stream. A suitable reference point, suggested by the model, is the crossing of the isopycnal $\tilde{\gamma} = 0.4$ at $z^*/\bar{D} = 0.35$. From the model results in Figs. 1a and 1b, it is seen that the x^*-location of this point is also the location, at the surface, of the maximum surface ve-

TABLE 2. Values of various parameters for sections I, II and III of Gulf Stream '60. λ and $\bar{L}$ are generated by the model.

Gulf Stream '60 section number	Longitude (W)	Δh_m (m)	λ (km)	$\bar{L}$ (km)	$\bar{D}$ (m)
Section I	68°30'	1.18	70	116	1375
Section II	66°30'	0.95	110	182	1330
Section III	64°30'	1.00	91	150	1450

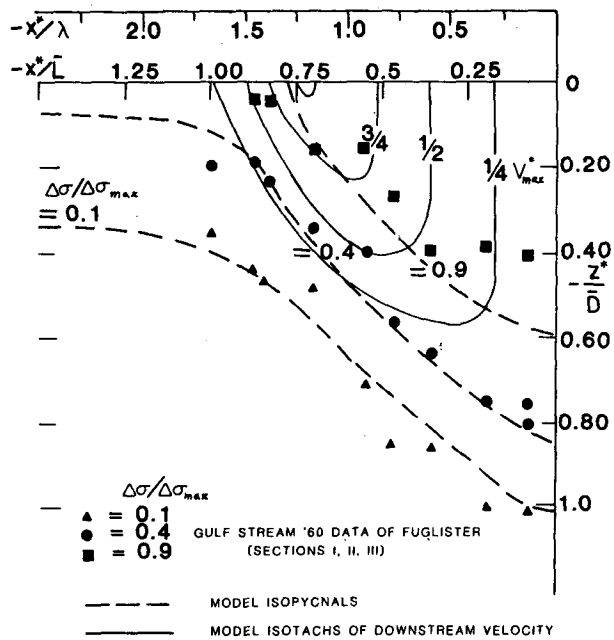

FIG. 4. Comparison between model-generated isopycnals, shown as dashed lines, for $\Delta\sigma$ = 0.1, 0.4 and $0.9(\Delta\sigma)_m$ and data from all three sections of Fuglister's Gulf Stream '60 experiment in the frontal region. ▲ data for $0.1(\Delta\sigma)_m$, ● data for $0.4(\Delta\sigma)_m$, ■ data for $0.9(\Delta\sigma)_m$. Also shown are the model-generated downstream velocity isotachs for v^* = ¼, ½, ¾ and $1v_m^*$, shown as solid lines.

locity. It will be seen below that the reference point so chosen corresponds to the location at which the 10° isotherm crosses ~500 m for data types (i) and (iii) above. For data type (ii) the approximate location of the maximum surface velocity was used, and minor adjustments were made to give the best fit to the dataset.

Figures 3a, b and c show the isopycnals from three transects (sections I, II and III) computed from Fuglister's Gulf Stream '60 data (Fuglister, 1963). All three sections are approximately perpendicular to the Stream direction. The isopycnals are drawn for constant values of $\Delta\sigma/(\Delta\sigma)_m$, where $(\Delta\sigma)_m$ denotes the maximum deficit in sigma-t values between the Sargasso Sea water and deep water compiled from Fuglister's salinity and temperature data. Thus, $(\Delta\sigma)/(\Delta\sigma)_m$ = 0.1, 0.4 and 0.9 represent, respectively, isopycnals with 10%, 40% and 90% of $(\Delta\sigma)_m$.

The procedure for the analysis leading to the scaling length λ is as follows: from the density field, we calculate first the sea-surface height anomaly across the front using 1500 m as the reference level. From the sea-surface height profile, we then estimate the value of the maximum slope of the profile, $(dh/dx)_m$, and the maximum height change across the anomaly, Δh_m. From these λ is obtained according to (20) and (21). Then, λ is used to normalize the cross-section distance x^* as shown. For the vertical scale, $\bar{D}$, we use the depth of the isopycnic $(\Delta\sigma)/(\Delta\sigma)_m$ = 0.1 on the Sargasso Sea side of the front. The values of Δh_m, λ, $\bar{L}$, and $\bar{D}$ are tabulated in Table 2 for the three sections. We also note that in all these sections, the field value of g' as defined in the model is $(1.5 \pm 0.1) \times 10^{-2}$ m s^{-2}. It is seen from the figures that in each case the sloping isopycnals that form the "North Wall" of the Gulf Stream are spanned very well by a distance of approximately 2λ. It should also be noted that the isopycnal $\Delta\sigma = 0.4(\Delta\sigma)_m$ coincides with the 10°C isotherm to a remarkable degree of precision. An adequate correspondence of the 5°C isotherm and the isopycnal $\Delta\sigma = 0.1(\Delta\sigma)_m$ is also found. Fuglister's station numbers for the different sections are also indicated in the figures.

TABLE 3. Model-generated quantities for different values of input parameters from Seasat altimeter data.

Seasat pass number	Input parameters		Model-generated quantities			
	v_m^* (m s^{-1})	Δh_m (m)	λ (km)	$\bar{L}$ (km)	$\bar{D}$ (m)	Q_e (m^2 s^{-1})
234-A	1.50	1.40	100	165	1310	12
242-D	2.45	1.80	81	134	1680	53
277-A	3.55	1.45	44	73	1355	160
478-A	1.90	1.95	110	182	1820	25
486-D	1.30	1.10	91	150	1030	8
521-A	2.55	2.05	89	147	1915	60
564-A	1.20	1.00	89	147	935	6
572-D	2.35	1.15	55	91	1075	46
1181-A	2.00	1.30	71	117	1215	29
1224-A	2.65	1.30	52	86	1215	67
1267-A	2.45	1.65	73	120	1540	53
1310-A	2.65	1.40	58	96	1310	67
1353-A	1.55	1.40	100	165	1310	13
1396-A	1.45	1.45	110	182	1355	11
1439-A	2.00	1.40	76	125	1310	29
1482-A	1.90	1.40	79	130	1310	25
Mean	2.09	1.45	80	132	1355	42
Standard deviation	0.60	0.28	20	33	260	40

The station data from all three sections are now plotted against the model-generated front isopycnals in Fig. 4. Note that in Fig. 4 the cross-stream coordinate is now linear. In Fig. 4 the dashed lines represent model-generated isopycnals, and the symbols are Fuglister's field data from all three sections. The agreement is found to be good in a quantitative sense, although the isopycnal representing $\Delta\sigma = 0.9(\Delta\sigma)_m$ is found to be consistently shallower in the Sargasso Sea than the model-generated isopycnal of the same value. The thicker pycnocline, in turn, makes Δh_m calculated from the field data smaller by 30% on the average than the model estimate given by (15). Also shown in Fig. 4 are the model-given isotachs of ¼, ½, ¾ and $1v_m^*$, indicated by the solid lines. No measured velocity data was given by Fuglister.

We next turn to the comparison of the sea-surface height profile between the model and field data. As mentioned earlier, the sea-surface height profiles from Fuglister's three sections were compiled. In addition, 16 sea-surface height profiles are available from the Seasat altimetry data analyzed by Cheney and Marsh (1981). The data cover the same region of the North Atlantic between 65° and 72°W. The sea-surface height data were derived from subtracting the best available geoid, namely, the Marsh–Chang geoid, from the direct altimetric height measurements. The degree of precision of the Seasat altimeter was 5–8 cm. For all the passes analyzed in the paper, the angle of intersection of the satellite ground track and the Gulf Stream axis has been estimated by Cheney and Marsh (1981) to be greater than 65°, implying less than 10% error due to the angle of intersection. These authors also estimated the values of the maximum height change Δh_m across the Gulf Stream and the maximum velocity v_m^*. These values are given in Table 3. Also included in Table 3 are the values of λ computed from (20). (These values have been given by Kao, 1982, in a brief note.) Table 3 gives values of the Gulf Stream width, $\bar{L}$, as given by (22), the values of $\bar{D}$ as given by (15), and the model

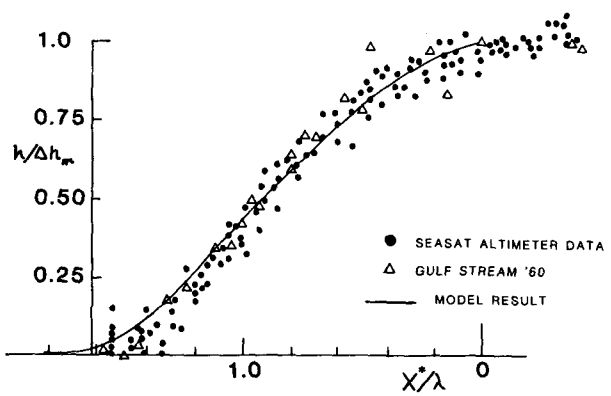

FIG. 5. Comparison between model-generated normalized sea-surface height profile across the Gulf Stream, shown as solid line, and (i) Seasat altimetry data, ●; (ii) reconstructed Gulf Stream '60 data from all three sections, △.

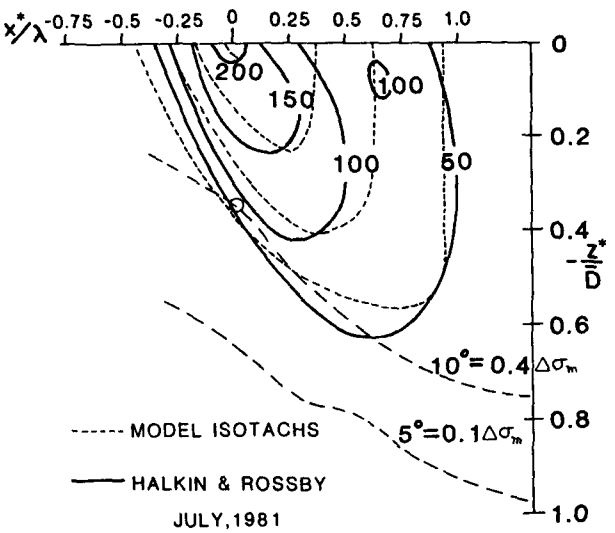

FIG. 6. Comparison between model-generated downstream velocity isotachs, shown as short dashed lines, and HR's directly measured downstream velocity isotachs of July 1981 at 73°W using the Pegasus profiler, shown as solid lines. Also shown are the locations of the measured 10° and 5°C isotherms. Numbers on the measured isotachs denote velocity in cm s^{-1}. (λ = 78 km from model.)

inflow, Q_e, as given by (13). The mean and standard deviations of the various quantities are also shown in Table 3. The standard deviation is in the range of 20% to 30% in all the quantities except Q_e, which has a higher standard deviation of approximately 100% of the mean. It is thus seen that if the values of Δh_m and v_m^*, estimated by using the best available geoid, are sufficiently accurate representations of their true values, then the subsurface structure of the Gulf Stream is completely determined from the model.

It is now possible to compare the model profile with the sea-surface height profiles from the detailed Seasat data and the reconstructed profiles from Fuglister's sections I, II and III. This comparison is shown in Fig. 5 for the normalized profiles. The solid line is the model profile. The solid dots indicate data from six Seasat crossings previously analyzed by Kao and Cheney (1982). It should be emphasized that it is the normalized profile that is being plotted, so that the agreement in height is less significant than the fact that, in spite of the variability of the widths of the Gulf Stream, the Gulf Stream is rather precisely spanned by 1.65λ as demanded by the model.

So far, the comparisons are restricted to the subsurface density structure. Direct velocity structure of the Gulf Stream is extremely difficult to obtain. It is indeed fortunate that Halkin and Rossby (1985; hereafter referred to as HR) have presented high-quality velocity data for a section centered at 73°W. The data were obtained by means of a free-falling velocity profiler, the Pegasus, developed by Rossby and Dorson of the University of Rhode Island. Halkin and Rossby gave data for both the downstream velocity and the cross-stream velocity (e.g., see the March 1982 data given in

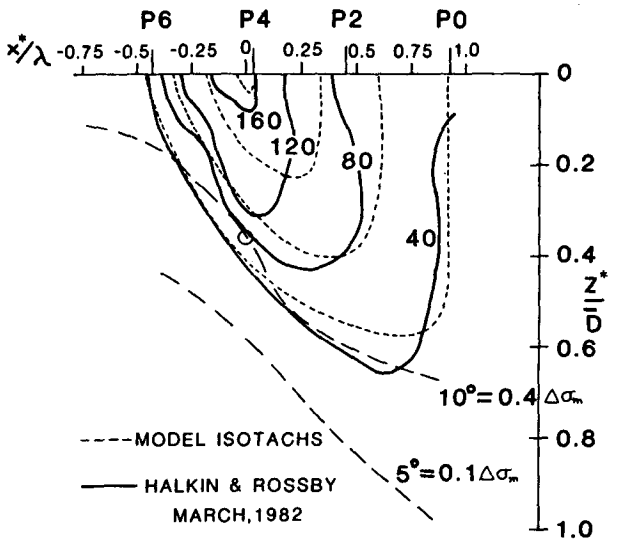

FIG. 7. As in Fig. 6 but for March 1982. (λ = 100 km).

Fig. 6 of HR). It is therefore possible to make a detailed quantitative comparison of the model isotachs with the field data for a representative transect. Since figures representing the downstream and cross-stream isotachs data of July 1981 were available to the author, a detailed comparison will also be made against those data.

The maximum measured downstream baroclinic velocity was defined in HR as the directly measured downstream velocity minus the downstream velocity at 2000 m. Halkin and Rossby also defined a "stream coordinate" system in which the x-axis was the cross-stream coordinate and the y-axis was along the Stream. The x-coordinate was positioned relative to a reference point halfway between where the 12° isotherm crossed 400 and 600 m. The reference point so defined is very close to the reference point defined earlier in this paper. For the July 1981 data, the maximum measured baroclinic velocity v_m^* was 1.9 m s^{-1} and the asymptotic depth of the 5°C isotherm on the Sargasso Sea side was approximately 1400 m, so that $\bar{D}$ is taken to be 1400 m. For the March 1982 data given in HR, v_m^* = 1.45 m s^{-1}, and $\bar{D}$ is again placed at 1400 m. For these input values of v_m^* and $\bar{D}$, the model results for July 1981 give $\bar{L}$ = 130 km from (14), λ = 78 km from (22), Q_e = 24 m^2 s^{-1} from (13), and the total baroclinic transport, Q = 82 Sv, from (24). For March 1982, $\bar{L}$ = 170 km, λ = 100 km, Q_e = 11 m^2 s^{-1}, and Q = 82 Sv. Using λ as the reference horizontal length and $\bar{D}$ as the reference depth, HR's July 1981 data and March 1982 data for the isotachs of the downstream velocity are reproduced in Fig. 6 and Fig. 7, respectively. The measured isotachs are shown as solid lines, with the numbers denoting the magnitudes in centimeters per second. The locations of the 10° and 5°C isotherms are indicated by the dashed lines. The reference point for the x^*-coordinate is indicated by a circle. This reference point is where the 10°C isotherm crosses 500 m. The origin of the x^*-coordinate is as indicated in the figures. The dotted lines indicate the model-predicted isotachs of the same magnitude. It is seen that the agreement is excellent even though there is, in the top 200 m, an increase in velocity downward to the right of the surface maximum in the July 1981 data. This feature is much less pronounced in the March 1982 data given in HR. For that case this downward

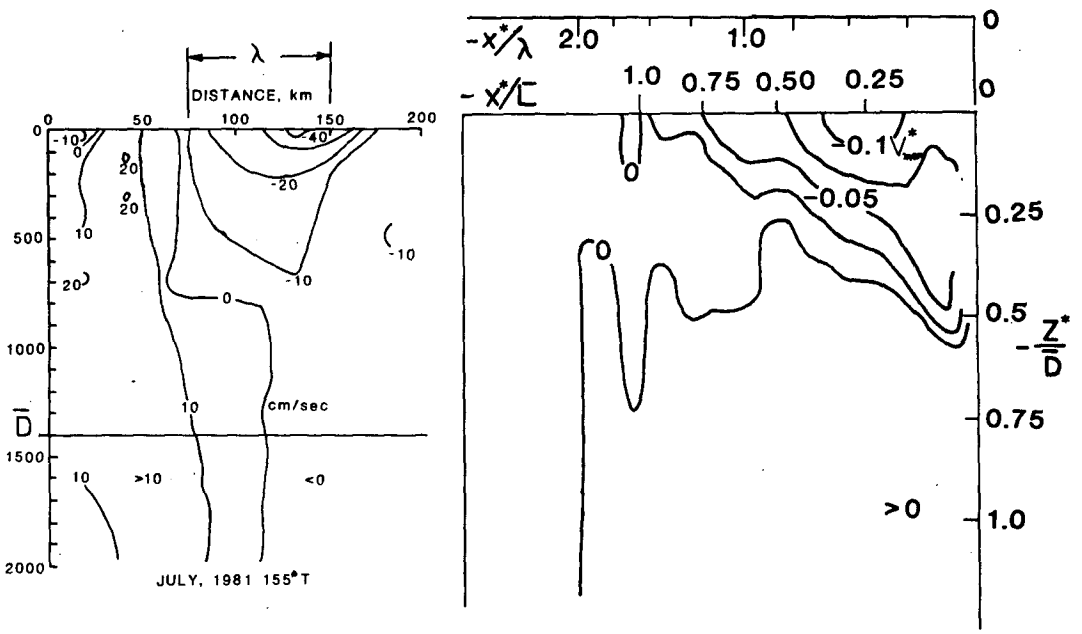

FIG. 8. Comparison between model-generated cross-stream velocity isotachs and typical field data (July 1981) of HR. The field data are shown in the left half of the figure.

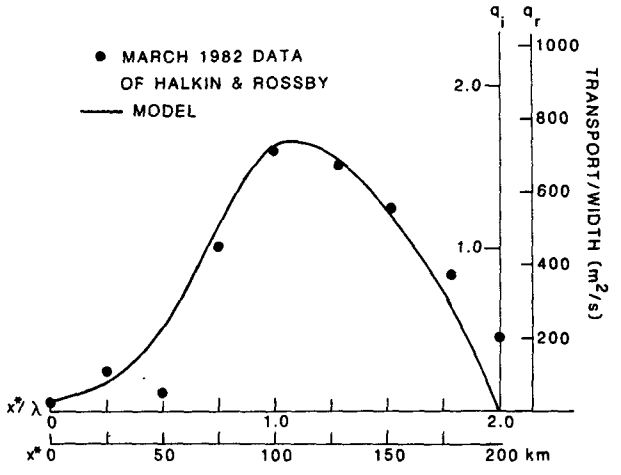

FIG. 9. Comparison between model-generated dimensional downstream baroclinic transport per unit width and data of March 1982, given in Fig. 7 of HR. (λ = 100 km from model.)

increase occurs very weakly at stations P2 and P3. An examination of the near-surface isotherms in the same figure reveals a weak cold-core eddy at P2, which could perhaps explain the weakening of the downstream velocity at the surface at P2 and P3 and an increase of the surface velocity at P1. What is perhaps an even more important comparison is the cross-stream velocity isotachs, since the cross-stream velocity is the manifestation of the inflow. This comparison is shown in Fig. 8 for the July 1981 data. The cross-stream velocity toward the front from the Sargasso Sea side in the field data shows marked similarity to the model result. However, the field data does not indicate an outflow at greater depths on the offshore side, even though the cross-stream velocity at or below the main thermocline level becomes very weak. The March 1982 data given in Fig. 6c of HR, on the other hand, does indicate a small positive (>0) value (i.e., outflow) below 900 m. In any case, the deep cross-stream velocities are small and somewhat uncertain in the field data. (Additionally, convergent flow from the slope water side of the Gulf Stream noted by HR was not present in the model. It should be stated that, since the slope water inflow carries no density deficit, it would not affect the dynamics of the Gulf Stream.) As noted above, the inflow from the Sargasso Sea side for the July 1981 data was found from the model to be 25 $m^2\ s^{-1}$ or 2.5 Sv per 100 km, which compares favorably with the mean value 5.0 Sv per 100 km with a standard deviation of 3.8 Sv per 100 km stated in HR. The mean and standard deviations of Q_e given by HR are closely comparable to the Seasat values estimated through the use of the model as shown in Table 3. The total baroclinic transports for July 1981 and March 1982 from the model are both 82 Sv, which are again in excellent agreement with the values given in Fig. 13 of HR. Comparison of the model transport per unit width with the field data given in Fig. 7 of HR for the March 1982 data is also possible. This is shown in Fig. 9 of the present paper. The agreement is seen to be remarkably good in the absolute quantitative sense.

5. Concluding remarks

The favorable comparison with the three different types of high-quality field data suggests that the dynamics of the Gulf Stream is indeed governed by the ageostrophic inflow from the Sargasso Sea as postulated in the present model. The similarity nature of the Gulf Stream data is truly impressive in spite of the variability of the Stream in terms of its width, depth, maximum velocity, and transport. The variability is largely associated with the meanders and instabilities of the Stream. These meanders and instabilities, in turn, often lead to the formation of warm- and cold-core eddies. The study of the meanders and instabilities and the subsequent pinch-off and formation of eddies is, of course, beyond the scope of the present paper. Nonetheless, the model provides the means of associating the whole-current structure with some simpler observations. Its utility as a diagnostic tool, in the sense just stated, has been demonstrated in this paper. Indeed, the model requires only two input parameters for the complete determination of the subsurface structure when eddy formation is not incipient: (i) either the asymptotic depth of the 5°C isotherm in the Sargasso Sea, $\bar{D}$, or the maximum sea-surface height rise across the stream, Δh_m, and (ii) the maximum surface velocity, v_m^*. Furthermore, if a reliable sea-surface height profile across the stream is available from satellite-borne altimeter measurements, v_m^* and Δh_m are easily extracted from the measurements, and hence, complete Gulf Stream structure information can be derived from the model.

Acknowledgments. The support of the Physical Oceanography program, Office of Naval Research, under Contract N00014-82-K0676 is gratefully acknowledged. The author is also indebted to the referees who provided constructive criticisms that led to substantial improvements in the presentation of the results.

REFERENCES

Cheney, R. E., and J. G. Marsh, 1981: SEASAT altimeter observations of dynamic ocean currents in the Gulf Stream region. *J. Geophys. Res.*, **86**, 473–483.

Fuglister, F. C., 1963: Gulf Stream '60. *Progress in Oceanography*, Vol. 1, M. Sears, Ed., Macmillan, 265–373.

Halkin, D., and T. Rossby, 1985: The structure and transport of the Gulf Stream at 73°W. *J. Phys. Oceanogr.*, **15**, 1439–1452.

Hurlburt, H. E., 1984: The potential for ocean prediction and the role of altimeter data. *J. Mar. Geodesy*, **8**, 17–66.

Kao, T. W., 1980: The dynamics of oceanic fronts. Part I: The Gulf Stream. *J. Phys. Oceanogr.*, **10**, 483–492.

——, 1983: Physical aspects of a length scale for the Gulf Stream front. *J. Geophys. Res.*, **88**, 6067–6068.

——, and R. E. Cheney, 1982: The Gulf Stream front: A comparison between SEASAT altimeter observations and theory. *J. Geophys. Res.*, **87**, 539–545.

Stommel, H., 1965: *The Gulf Stream.* 2nd ed., University of California Press.